Carbohydrate Polymer Technologies and Applications 1 (2020) 100012

Contents lists available at ScienceDirect

Carbohydrate Polymer Technologies and Applications

journal homepage: www.elsevier.com/locate/carpta

Use of thermodynamics in understanding drug release from xanthan gum matrices: The influence of clay-drug complexes ☆

A.M. Totea [a], I. Dorin [b], P.R. Laity [c], B.R. Conway [a], L. Waters [a], K. Asare-Addo [a,*]

[a] School of Applied Sciences, Department of Pharmacy, University of Huddersfield, Queensgate HD1 3DH, Huddersfield, United Kingdom
[b] Biomolecular Formulation and Characterization Sciences, UCB, Slough SL3WE, United Kingdom
[c] Department of Materials Science and Engineering, University of Sheffield, Sir Robert Hadfield Building, Mappin Street, Sheffield S1 3JD, United Kingdom

ARTICLE INFO

Keywords:
Complexation
Isothermal titration calorimetry
Magnesium aluminium silicate
Propranolol hydrochloride
Xanthan gum

ABSTRACT

The aim of this study was to outline a novel way of understanding the controlled drug release from drug-clay-polymer matrices using isothermal calorimetry (ITC) as a complementary technique to dissolution studies. ITC results showed that the binding phenomenon between the model drug propranolol hydrochloride (PPN) and magnesium aluminium silicate (MAS) in the presence of xanthan gum (XG was spontaneous and enthalpically driven (negative enthalpy (ΔH) and small entropy (-TΔS)). This may be due to the competition for PPN due to the anionic nature of XG. Dissolution results showed that when using the MAS-PPN complexes, 10% w/w XG polymer level was enough to significantly reduce the burst release. When used together, ITC and dissolution studies may help a formulator understand and identify interactions which occur during dissolution studies and may be beneficial to the controlled drug delivery system.

1. Introduction

Minerals have physicochemical properties such as chemical inertness, high adsorption capacity and specific area, swelling, water solubility and dispersivity, plasticity, acid-absorbing capacity, as well as colour, opacity and low or no toxicity in patients, which makes them suitable for medical and pharmacological applications (Carretero, 2002; Carretero & Pozo, 2009). In the formulation of pharmaceutical dosage forms, minerals can be used as excipients, carriers of active ingredients to achieve modified release, as binders, fillers, disintegrants, lubricants, thickening agents, anticaking agents, flavouring correctors and emulsifying agents. The use of minerals as drug carriers in the formulation of pharmaceutical dosage forms has gained more interest in the development of controlled drug release systems. Minerals are able to adsorb or reversibly fixate polar compounds onto their structure and form complex dispersions and particles, which can, in turn, modify the release of drugs upon administration (Carretero & Pozo, 2009). Modified drug release is particularly desirable for drugs used to treat chronic conditions that have a short half-life and require frequent administration to maintain adequate drug plasma levels (Rojtanatanya & Pongjanyakul, 2010).

The most widely used smectite clays used within the pharmaceutical industry are montmorillonite, saponite and hectorite, often used as excipients within drug formulation. These share structural similarities but have unique chemical compositions. Magnesium aluminium silicate (MAS) is a mixture of natural smectite montmorillonite and saponite clays, having a layered silicate structure, formed of one alumina or magnesia octahedral sheet, sandwiched between two tetrahedral silicate sheets (Fig. 1) (Kanjanakawinkul, Rades, Puttipipatkhachorn & Pongjanyakul, 2013). MAS has a high surface area, a very good affinity with cationic drugs and it is not toxic or an irritant.

Numerous studies have aimed to form intercalated complexes through the adsorption of different compounds such as (nicotine (NCT) and propranolol hydrochloride (PPN)) onto MAS as well as polymers such as chitosan (CS) (Kanjanakawinkul et al., 2013; Khunawattanakul, Puttipipatkhachorn, Rades & Pongjanyakul, 2010; Pongjanyakul & Rojtanatanya, 2012; Pongjanyakul, Khunawattanakul & Puttipipatkhachorn, 2009; Rojtanatanya & Pongjanyakul, 2010; Rongthong, Sungthongjeen, Siepmann & Pongjanyakul Quaternary, 2013). The formed complexes and composites were essentially used to

Abbreviations: MAS, Magnesium aluminium silicate; PPN, Propranolol hydrochloride; ITC, Isothermal titration calorimetry; SIM, Single injection mode; MIM, Multiple injection mode; HPLC, High performance liquid chromatography; RSD, Relative standard deviation; XG, Xanthan gum; HCl, Hydrochloric acid; RPM, Rotations per minute; MDT, Mean dissolution time; MDR, Mean dissolution rate; NCT, Nicotine; CS, Chitosan.

☆ Submission: Carbohydrate Polymer Technologies and Applications

* Corresponding author.
E-mail address: k.asare-addo@hud.ac.uk (K. Asare-Addo).

https://doi.org/10.1016/j.carpta.2020.100012
Received 11 June 2020; Received in revised form 12 October 2020; Accepted 15 October 2020
Available online 20 October 2020

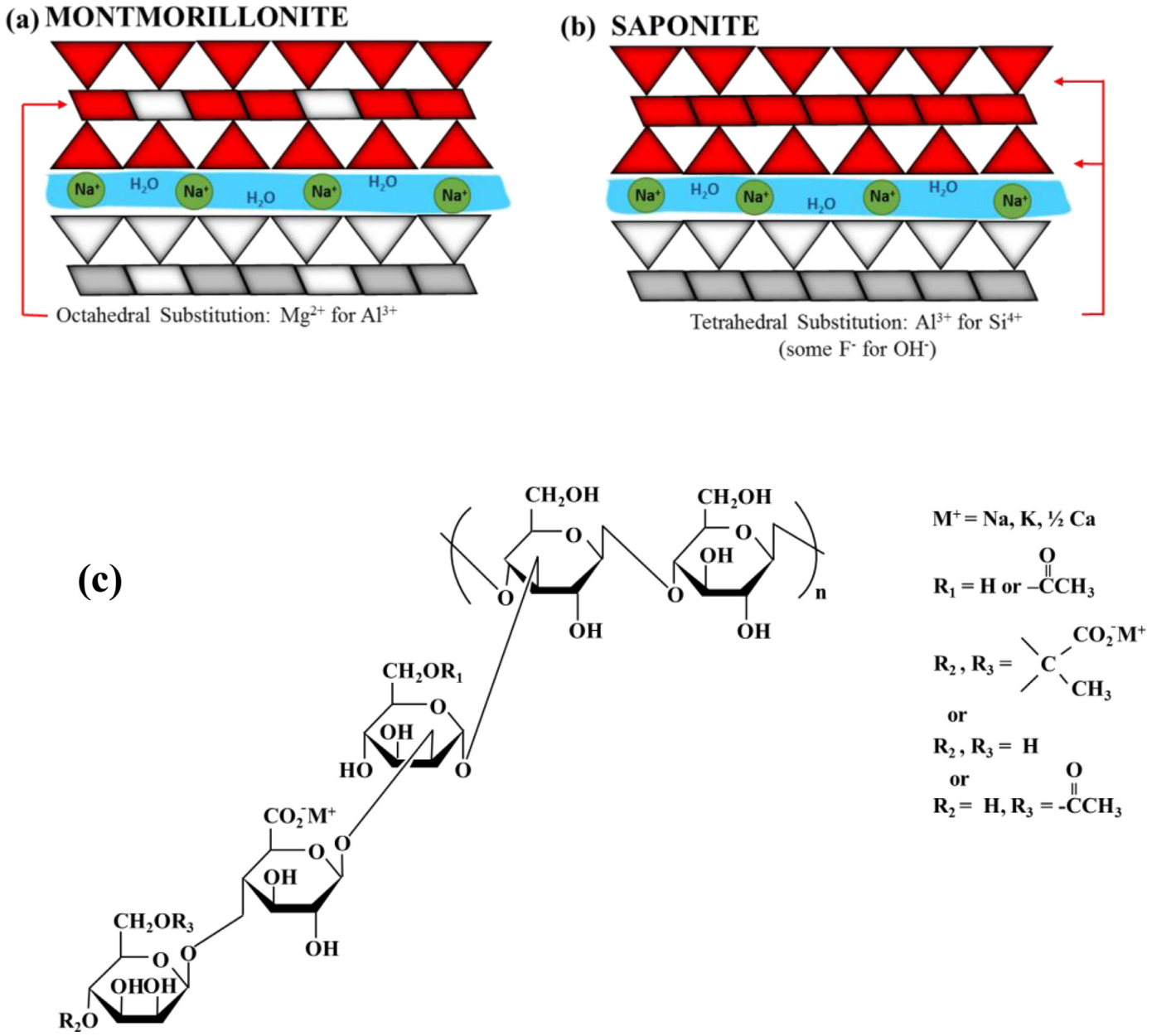

Fig. 1. Structure of montmorillonite (a) and saponite (b) clays found in MAS, showing the magnesia or alumina octahedral sheet trapped between two tetrahedral silicate sheets: adapted from Vanderbilt Minerals, 2014, (c) chemical structure of XG: adapted from (CPKelco, 2008).

modulate drug release. Multiple other studies published using smectite clays showed their capacity to adsorb a wide variety of drugs and form complexes able to modulate drug release. Drugs such as chlorhexidine acetate, timolol maleate, donepezil, sertraline hydrochloride, theophylline, tetracycline, diltiazem hydrochloride, nicotine and diclofenac sodium were shown to be adsorbed onto montmorillonite and form complexes (Adebisi, Conway & Asare-Addo, 2015; Asare-Addo, Totea & Nokhodchi, 2020; Joshi, Kevadiya, Patel, Bajaj & Jasra, 2009; Kaur & Datta, 2014; Meng, Zhou, Zhang & Shen, 2009; Muśko & Sznitowska, 2013; Nunes et al., 2007; Okeke & Boateng, 2016; 2017; Park et al., 2008; Parolo, Savini, Valles, Baschini & Avena, 2008; Trivedi, U, Maniruzzaman & Coleman, 2018) and exploited for drug delivery. Totea et al. also aimed to understand the binding process of diltiazem hydrochloride and propranolol hydrochloride onto MAS using isothermal titration calorimetry. The studies confirmed the binding and offered insight into thermodynamics of the binding process (Totea et al., 2019; 2020a; 2020b).

PPN is the model drug of choice in this study and was adsorbed onto MAS to form complex dispersions and particles aimed to modulate drug release. PPN is a highly soluble β-blocker, which has its therapeutic effect from antagonizing the adrenergic pathway that can lead to blocking receptors in heart, lungs, liver, pancreas, peripheral blood vessels and other parts of the body. PPN is efficient in the treatment of high blood pressure, angina pectoris and myocardial infarction, as well as severe infantile haemangioma (Guan et al., 2015). PPN's drawback is the short half-life of 3.9 h which requires frequent administration 2–3 times/day, therefore making it a suitable target for controlled drug release formulation.

XG is a polysaccharide having a repeating unit consisting of five sugar residues: one glucuronic acid, two glucose and two mannose. The

polymeric chain is identical to cellulose, consisting of 1, 4-linked ß-D-glucose. The distinguishable component from cellulose is the trisaccharide side backbone consisting of alpha-D-mannose typically containing a linked acetyl group, beta-D-glucuronic acid and a terminal beta-D-mannose usually linked to a pyruvate group (Fig. 1c) (CP Kelco KELTROL® / KELZAN® xanthan gum book, 2008). XG can be efficiently used as an excipient in the formulation of dosage forms for intended controlled drug delivery. XG is a hydrophilic matrix polymer normally used in small amounts in the formulation of tablets due to its efficiency. When tablets get into the dissolution media (i.e. stomach, small intestine), the XG particles on its surface become hydrated and form a gel layer which is viscous and enables drug diffusion but is resistant to erosion. XG has been shown to provide time-independent release (Jian, Zhu, Zhang, Sun & Jiang Galactomannan, 2012). These therapeutic advantages led to the use of XG in numerous published studies as an excipient in tablets to control drug release (Andreopoulos & Tarantili, 2001; CP Kelco KELTROL® / KELZAN® xanthan gum book, 2008; Jian et al., 2012; Lazzari, Kleinebudde & Knop, 2018; Petri, 2015; Talukdar & Kinget, 1995; Talukdar, Michoel, Rombaut & Kinget, 1996).

Although numerous studies have demonstrated XGs efficacy in controlling drug release on its own or in combination with other polymers (Nokhodchi, Palmer, Asare-Addo, Levina & Rajabi-Siahboomi, 2015), XG has never been used in combination with MAS to the best of our knowledge. The present study therefore firstly aims to evaluate the effects on controlling PPN release from a combination between a polymer, XG and MAS-PPN complexes or physical mixtures. We also report for the first time the thermodynamics using isothermal calorimetry (ITC) to give insights into the complexation process at the molecular level which may impact drug release.

Hypothesis: Binding between MAS and PPN will be more enthalpy driven in the presence of XG due to competition for PPN thus affecting the binding at the molecular level and have consequences on the drug release.

2. Material and methods

2.1. Materials

VEEGUM F EP® or magnesium aluminium silicate (MAS) was a kind gift from R.T.Vanderbilt Company, Norwalk, CT (USA). Xanthan gum (XANTURAL® 75) was also a kind donation by CP Kelco Ltd. (Leatherhead, UK) and has a molecular weight of approximately 2000,000 Da (CP Kelco KELTROL® / KELZAN® xanthan gum book, 2008 and Ferstl et al., 2013). The viscosity as measured using a Kinexus rheometer, Malvern Instruments, Herrenberg, Germany of the 0.1% (w/w) xanthan gum solution in 0.1 N HCl at 37 °C with a rotational rheometer equipped with a cone plate system (angle of the cone: 1°) was 5.5 mPa s (Lazzari et al., 2018). It is important to note that the extraction methodology that produces differences in the molecular weight and viscosity grades of xanthan gum (Wang, Wu, Zhu & Zhan, 2016, 2017) can impact and influence drug release. Propranolol hydrochloride (PPN) was purchased from TCI (Tokyo Chemical Industry, Tokyo). Acetonitrile (HPLC grade), sodium phosphate dibasic dihydrate, 99+% (HPLC grade), sodium hydroxide and 2 M hydrochloric acid were purchased from Fisher Scientific (UK).

2.2. Methods

2.2.1. Formulation of MAS-PPN complex particles

The MAS-PPN complex particles were prepared as reported in Totea et al., 2019 using MAS dispersions (2% w/v) and PPN solutions (2% w/v). The double loaded MAS–PPN complex dispersions obtained after the drying process were milled (Retsch® PM 100 Ball Mill set at 350 rpm) and the particle size fraction of 65–123 μm stored in a glass vial and used as needed.

2.2.2. Attenuated total reflectance Fourier transform infrared spectroscopy (ATR-FTIR)

ATR-FTIR (Smart Orbit ATR-FTIR) was used to characterise potential molecular interactions between MAS and PPN using diamond as the ATR crystal scanned from 4000 to 400 cm^{-1}.

2.2.3. Scanning electron microscopy/ energy dispersive X-ray spectroscopy (SEM/EDX)

SEM (QUANTA FEG 250 microscope) was conducted to elucidate the surface morphology of the samples to detect potential changes that may have occurred following the complexation process. PPN, MAS or the complex was mounted on a metal stub with double-sided adhesive tape and sputter coated with a thin layer of gold. The micrographs of the samples studied were taken at various magnifications at 20 kV.

2.2.4. Differential scanning calorimetry (DSC)

1–10 mg of PPN, MAS or the complex was placed onto a 40 μL aluminium crucible with the lid hermetically sealed and heated between 25 and 500 °C, at a rate of 10 °C/min using a DSC instrument (Mettler Toledo, Switzerland).

2.2.5. X-ray powder diffraction (XRPD)

Analysis of the PPN, MAS and complex was performed at an angular range 2.5–70° (2θ) and a step angle of 0.02° (2θ) s^{-1} using a D2 PHASER (BRUKER). The X-ray source was generated as a Cu radiation at 30 kV and 10 mA.

2.2.6. Drug content analysis from the MAS-PPN complexes using HPLC

Drug content within the MAS-PPN complexes was determined by dispersing 50 mg of the prepared complex particles in 100 mL of a 2 M HCl, ultra–pure water or pH 6.8 phosphate buffer under continuous stirring for 24 h, at 25 °C and 700 rpm and filtered using 0.2 μm syringe filters. The clear supernatant was analysed using reversed phase high performance liquid chromatography (Shimadzu HPLC, Japan), equipped with an SPD-20AV UV–Vis detector, using an XTerra® MS C18 150 mm × 4.6 mm × 3.5 μm column. The mobile phase was prepared using acetonitrile and 0.01 M sodium phosphate dibasic dihydrate (pH 3.5) at a ratio of 30:70 v/v. The flow rate of the mobile phase was set at 1 mL/min with a detection wavelength of 230 nm.

2.2.7. Tablet preparation and bulk compaction behavior

The powder mixture required to make the tablets containing MAS-drug complex was prepared by mixing the amount of MAS-PPN complex equivalent to a set amount of active ingredient (i.e. 40 mg PPN) with XG at a ratio of 1:1 w/w. The powder mixture required to make the tablets containing MAS-drug physical mixture and XG was prepared using the same amounts of powder as in the tablets containing MAS-drug complex particles (equivalent to a set amount of active ingredient) (Table 1). The powder combination was mixed in a 3-D shaker/mixer Turbula T2F (Stort Eskens Ltd., UK) for 10 min. The powder mixture was poured into the die and tablets were formed by applying a set force of 10 kN. A pre-set maximum force was set at 16 kN. During the compression stage, the displacement was measured accurately through a short-travel extensometer by the movement of the cross head of the machine which was set at 3 mm min^{-1} while the lower punch remained fixed. After the set force was reached, the upper-punch was allowed to retract at a speed of 1 mm min^{-1}. The recorded displacement was corrected using the apparent displacement under load of the instrument that was determined by performing compaction as described above on the empty dye. Once the experiment finished and the force applied returned to zero, the specimens were ejected from the dye using the same instrument set at a speed of 10 mm/min. The weight, as well as diameter and height of the specimens were recorded immediately.

Table 1
Formulation codes for tablets prepared using MAS-PPN complexes or MAS-PPN physical mixture (both containing an equivalent of 40 mg PPN), and XG in different amounts (50%, 30%, 10% and 5% w/w) and their powder and compact properties.

Relative density								
Formulation	Polymer amount in formulation (% w/w)	*Formulation code*	True density (kg/m^3)	Uncompacted	At maximum pressure	After ejection	Elastic recovery (%)	Porosity (%)
MAS-PPN (phys. mix) + XG	5	*XG5%_PM*	2050.56 ± 12.40	0.35 ± 0.01	0.79 ± 0.02	0.72 ± 0.01	8.35 ± 1.11	23.22 ± 1.07
	10	*XG10%_PM*	1910.47 ± 2.97	0.36 ± 0.02	0.83 ± 0.01	0.76 ± 0.02	7.93 ± 1.15	17.24 ± 0.72
	30	*XG30%_PM*	1799.95 ± 5.77	0.43 ± 0.00	0.85 ± 0.01	0.79 ± 0.01	6.78 ± 0.23	15.58 ± 0.57
	50	*XG50%_PM*	1718.95 ± 2.65	0.45 ± 0.02	0.85 ± 0.00	0.80 ± 0.00	5.72 ± 0.08	13.50 ± 0.63
MAS-PPN (complex) + XG	5	*XG5%_C*	1952.43 ± 1.02	0.37 ± 0.01	0.81 ± 0.00	0.74 ± 0.00	7.59 ± 0.82	20.50 ± 0.46
	10	*XG10%_C*	1946.70 ± 1.87	0.37 ± 0.01	0.81 ± 0.00	0.76 ± 0.00	6.03 ± 0.33	20.31 ± 0.25
	30	*XG30%_C*	1855.78 ± 2.26	0.47 ± 0.01	0.83 ± 0.00	0.78 ± 0.01	5.50 ± 0.41	17.84 ± 0.74
	50	*XG50%_C*	1731.33 ± 1.26	0.47 ± 0.00	0.85 ± 0.00	0.80 ± 0.00	5.10 ± 0.23	16.09 ± 1.17

2.2.8. True density and porosity determination

The true density of the powder mixtures used to make tablets was determined by helium pycnometry on an AccuPyc II 1340 (Micrometrics, UK). The determination of the true density of the formulations (Table 1), along with the tablet weight, height and diameter allowed for the determination of tablet porosity (Eq. (1)) (Asare-Addo, Levina, Rajabi-Siahboomi & Nokhodchi, 2011).

$$\text{Tablet porosity} = \left[1 - \frac{\text{Tablet weight/Tablet volume}}{\text{True density of powder}}\right] x100 \quad (1)$$

2.2.9. Dissolution testing

The *in vitro* release characteristics of the tablets prepared were analysed using a USP dissolution apparatus with sinkers (paddle method; PT-DT70 Pharma Test, Germany). Tablets were tested in 900 mL of 0.1 M hydrochloric acid (pH 1.2) to simulate the gastric fluid for up to 9 h or 900 mL of phosphate buffer (pH 6.8) to simulate the intestinal fluid for up to 9 h. The rotation speed of the paddles was 100 rpm. Samples were collected automatically at suitable intervals and were analysed at a wavelength of 290 nm in each case by the UV–Vis detector attached to the dissolution instrument. All experiments were performed in triplicate for reproducibility.

2.5.1. Kinetics of drug release and dissolution parameters

The dissolution profiles obtained were described by the Peppas model also known as power law and was used to determine the release mechanism based on the value of the diffusional exponent (Eq. (2)) (Dash, Murthy, Nath & ChowdhuryKinetic, 2010; Romero et al., 2018; Siahi-Shadbad, Asare-Addo, Azizian, Hassanzadeh & Nokhodchi, 2011).

$$Q = ktn \quad (2)$$

where Q is the percentage of drug released at time t, k is the release rate constant which describes the structure and geometry of the tablet, and n is the diffusional exponent which indicated the mechanism of drug release (Dash et al., 2010; Romero et al., 2018; Siahi-Shadbad et al., 2011). A value of n lower than 0.45 calculated from drug release of cylindrical tablets indicates Fickian diffusion mechanism. A value of n higher than 0.89 shows that the dissolution process was controlled by erosion and that the rate of drug release was independent of time, 'zero-order' release. An anomalous transport or non-Fickian is considered when n was between 0.45 and 0.89 which suggests that drug release is governed by both diffusion and erosion (Ritger & Peppas, 1987; Costa, Manuel & Lobo, 2001).

The efficiency on retarding drug release using PEO combined with both MAS-PPN complexes and physical mixtures were compared using the following equations describing the mean dissolution time (MDT) and the dissolution efficiency (DE – area under the dissolution curve up to a certain time t) (Eq. (3)) (Costa, Manuel & Lobo, 2001; Siahi-Shadbad et al., 2011).

$$MDT = \frac{\sum_{j=1}^{n} t\Delta M_j}{\sum_{j=1}^{n} \Delta M_j} \quad (3)$$

where j is the sample number, n is the number of dissolution sample times, t is the time at midpoint between t and t–1 (that can be calculated with the formula $(t + t - 1)/2$) and ΔM_j is the additional amount of drug that dissolved between t and t–1 (Costa, Manuel & Lobo, 2001; Siahi-Shadbad et al., 2011).

$$DE = \frac{\int_0^T Y \times dt}{Y_{100} \times T} \times 100\% \quad (4)$$

where Y is the percent of drug release at time t and Y_{100} represents 100% drug release (Costa, & Lobo, 2001; Siahi-Shadbad et al., 2011).

2.6. Calorimetric binding studies - effects of XG on the MAS-PPN interactions

To ascertain the effects of XG on the MAS-PPN complexes or how possible interactions between, drug, MAS and XG could inform the choice of formulation as well as the dissolution process, calorimetric MIM binding studies were carried out on the VP-ITC instrument (calibrated to ensure the instrument was within acceptable limits (Baranauskienė, Petrikaitė, Matulienė & Matulis, 2009)) at pH 5 and at two different temperatures (25 °C and 37 °C). A high-gain feedback mode whilst applying a reference power of 20 μcal s^{-1} under stirring at 307 rpm was used. The real-time binding isotherm was studied in 29–120 injections of 2–10 μL each into the sample cell every 260–550 s. XG dispersions were prepared separately using purified water under stirring at 500 rpm (25 °C) for 24 h. Each of the prepared dispersions was separately combined with one MAS dispersion and the resultant MAS-polymer complex was used in the sample cell. Fresh drug solution of PPN was added into the sample cell containing MAS-polymer complex (Table 2). All experiments were conducted in triplicate and the results analysed using Origin 7.0 (Microcal, Inc) software.

3. Results and discussion

3.1. Solid-state characterisation of complexed particles

MAS-PPN complexes have been evaluated and characterised previously (Pongjanyakul & Rojtanatanya, 2012; Totea et al., 2019). The results obtained from the SEM, FTIR, DSC and XRPD (Fig. 2) were in accordance with reported literature. SEM showed the incorporation of PPN into MAS to create MAS-PPN complex particles with changes in the microstructural properties of the MAS hence the possibility of the MAS-PPN complexes to control drug release (Fig. 2c) (Rapacz-Kmita, Krupa & Jachowicz, 2010). With regards to FTIR, the peak observed as the hydroxyl stretching belonging to Si-OH became smaller and shifted to a lower wavelength of 3631 cm^{-1} (Fig. 2d). The PPN adsorption onto

Table 2
Materials and parameters used in ITC SIM and MIM experiments.

Cell Clay/ polymer	Syringe Concentration (% w/v)	Number of injections Drug/polymer	Injection volume (μL) Concentration (% w/v)	Spacing (s)	Reference power (μcal/s)		
*MAS	0.037	PPN	0.15	1	150	2500	20
*MAS	0.037	PPN	0.15	120	2	260	20
MAS	0.037	XG	0.02	29	4	1200	10
XG	0.02	PPN	0.15	29	4	1200	10
MAS-XG	0.037 MAS 0.020 XG	PPN	0.15	120	2	260	10

*Experiment conducted and reported previously by Totea et al., 2019.

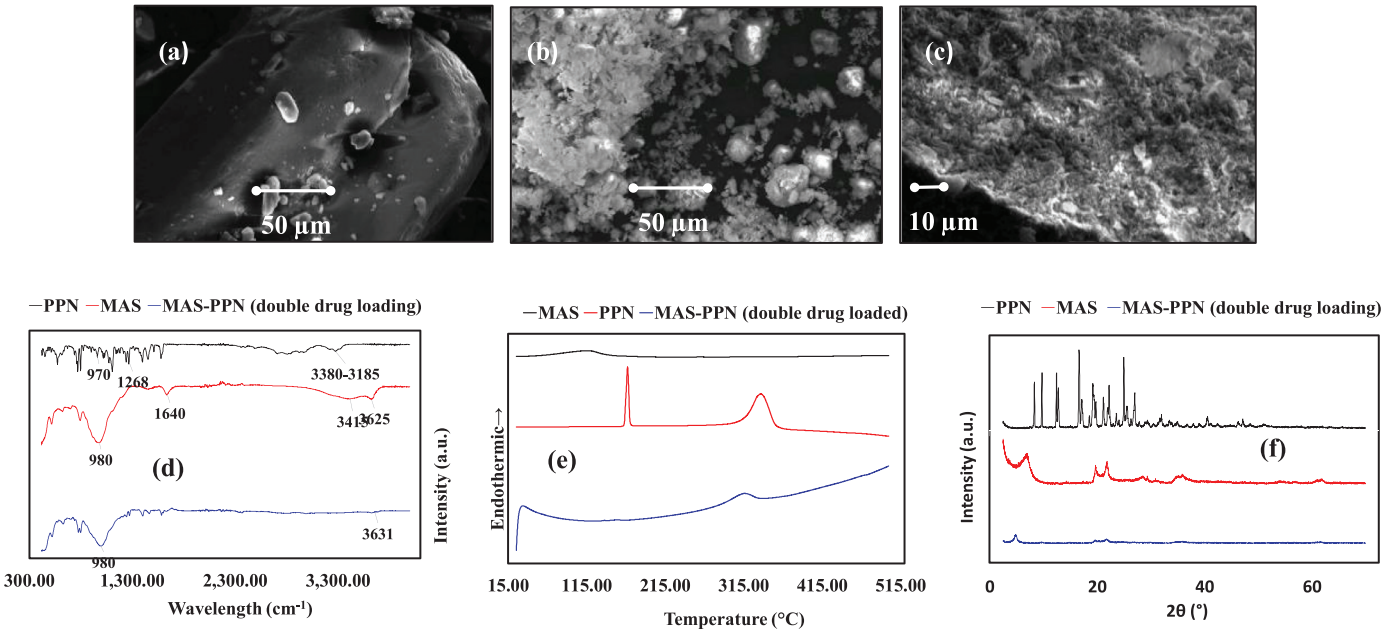

Fig. 2. SEM images of (a) PPN, (b) MAS, (c) MAS-PPN complex, (d) FTIR spectra of PPN, MAS and MAS-PPN complex, (e) DSC of PPN, MAS and MAS-PPN complex, (f) XRPD of PPN, MAS and MAS-PPN complex.

MAS was via hydrogen bond formation between the silanol groups of MAS with the amine and/or hydroxyl groups of PPN (Rojtanatanya & Pongjanyakul, 2010). The MAS-PPN complex particles prepared were shown to be amorphous and the absence of the melting point of PPN in the DSC profile confirmed that the drug was molecularly dispersed in the clay (Fig. 2e) (Rojtanatanya & Pongjanyakul, 2010). The XRPD data from Fig. 2f also suggested that the prepared MAS-PPN complexes contained molecularly dispersed PPN within the MAS due to the absence of the crystalline peaks of PPN (Rojtanatanya & Pongjanyakul, 2010; Sinha Ray, Maiti, Okamoto & Yamada, 2002).

3.2. Powder and tableting properties

Bulk compaction behavior was studied for the formulations prepared as plots of relative density vs. upper punch pressure measured during loading to 10 kN and unloading (Fig. 3). The compaction curves of all the samples tested followed roughly similar trends: the compaction behavior was dominated by plastic recovery during the loading stage following non-reversible deformation, movement and fragmentation of the particles (Laity & Cameron, 2008; Han et al., 2013; Laity, Asare-Addo, Sweeney, Supuk & Conway, 2015). Overall, the elastic recovery was considerably higher for the specimens containing a MAS-PPN physical mixture compared with those containing MAS-PPN complexes (Table 1). It was also noted that there was a decrease in the elastic recovery with an increase in the XG content, as the overall proportion of MAS in the tablets was reduced (Table 1). This behavior can be linked to the elastic recovery of MAS and was previously reported in literature by Laity et al. (2015)). The authors found that MAS exhibited significant elastic recovery upon compaction to 204 and 611 MPa which was attributed to changes in the basal spacing of the clay upon compaction or to the bending of the clay platelets (Laity et al., 2015). Hence, the overall reduction in elastic recovery during compaction upon use of MAS-PPN complexes and XG in the tablets instead of MAS-PPN physical mixture and XG is of high importance because it decreases the chances of tablets cracking, laminating or tooling wear (Laity et al., 2015). This trend was also observed for the porosity values for the physical mixture samples and complexed samples with the samples containing the complexes (with the exception of compacts with 5% XG content) generally having higher porosity at all polymer levels (Table 1). Tablet porosity values were calculated based upon sample volume and weight, as well as true density of the powder, the least parameter being an important differentiating factor in the results. This may be as a result of the physical mixture between MAS and PPN not being sieved to the same particle size as the complexes (used as supplied from manufacturers). On the other hand, the process of formulating the complexes involved a wide variety of procedures which led to different particulate physicochemical properties. Despite these differences between materials, porosity is an important parameter and overall, a higher porosity of tablets MAS-PPN complexes may offer additional benefits in controlling PPN release due to potential differences in water ingress. It is however important to note that other key tablet characteristics such as solubility, surface area and particle size can influence dissolution rates ("Micrometrics Porosity and Its Influence on Pharmaceutical Tablet Dissolution," 1998; Riippi et al., 1998).

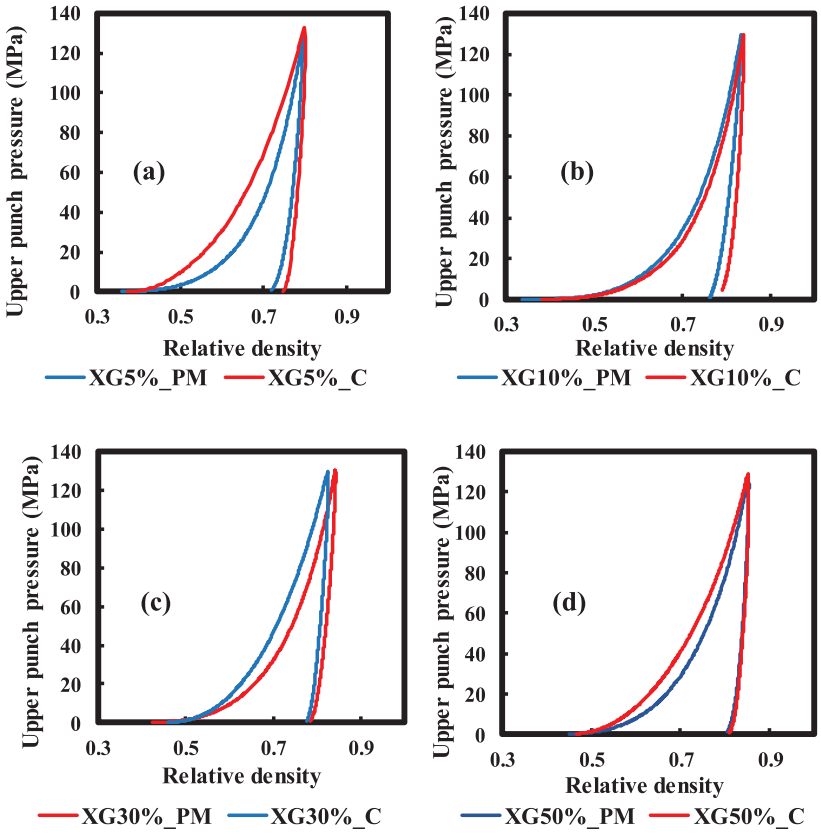

Fig. 3. Compaction behavior of formulations containing MAS-PPN complexes or MAS-PPN physical mixture compacted to 130 MPa: plots of measured upper punch pressure vs. relative density at (a) 5%, (b) 10%, (c) 30 and (d) 50% XG polymer content.

Table 3
Mechanism and kinetics of drug release of tablet matrices prepared using MAS-PPN physical mixture and MAS-PPN complexes incorporated in 5 - 50% XG polymer content.

Formulation	Dissolution media	Polymer amount in formulation (% w/w)	*Formulation code*	DE_{540min} (%)	MDT (min)	*n* value
MAS-PPN (phys. mix) + XG	pH 1.2	5	*XG5%_PM*	66.84	22.26	–
		10	*XG10%_PM*	65.89	54.62	0.62
		30	*XG30%_PM*	33.49	166.23	0.6
		50	*XG50%_PM*	22.93	226.67	0.68
MAS-PPN (complex) + XG	pH 1.2	5	*XG5%_C*	78.36	26.86	–
		10	*XG10%_C*	51.61	166.96	0.74
		30	*XG30%_C*	39.02	174.31	0.63
		50	*XG50%_C*	24.47	239.51	0.8
MAS-PPN (phys. mix) + XG	pH 6.8	5	*XG5%_PM*	62.87	18.85	0.56
		10	*XG10%_PM*	35.41	141.58	0.57
		30	*XG30%_PM*	23.02	219.43	0.81
		50	*XG50%_PM*	17.42	237.94	0.73
MAS-PPN (complex) + XG	pH 6.8	5	*XG5%_C*	64.53	76.37	0.73
		10	*XG10%_C*	30.69	180.77	0.63
		30	*XG30%_C*	24.59	200.68	0.69
		50	*XG50%_C*	17.02	252.01	0.79

3.3. Dissolution, dissolution parameters and kinetics of drug release

The use of XG in tablets in different amounts (5, 10, 30, 50% w/w) allowed the observation of MAS-PPN complexes and physical mixture behavior in combination with XG and its effects on modulating PPN release. At 5% XG w/w, PPN release was rapid for all the tablets tested (Fig. 4a and b). At pH 1.2, tablets containing MAS-PPN complexes and those containing MAS-PPN physical mixture were unable to retard PPN release, as they disintegrated within a few seconds. At pH 6.8, the tablets containing MAS-PPN complexes were shown to be relatively controlled compared with its physical mixture counterpart with a significant decrease in the initial burst release (Fig. 4b). What can also be observed here is the influence of ions in the dissolution media. It is important to note that XG is an anionic polymer. This therefore means the pH does have an influence on its behavior. XG has a pKa of 3.1 and hence, becomes less soluble at lower pH leading to a lower solubility and hence, a lower matrix swelling (Mu, Tobyn & Staniforth, 2003). Furthermore, the increase in ionic strength of the medium leading to a 'salting out' of the polymer causes the polymer to lose its water hydration properties and show a lower degree of swelling and erosion and form a more rigid structure (Kavanagh & Corrigan, 2004; Baumgartner, Pavli and Kristl, 2009).

The calculation of the *n* value was not possible for the dissolution of tablets containing 5% w/w XG and MAS-PPN complexes/ physical mixture in the acidic media due to the rapid PPN release. In buffer, the tablets had an anomalous (non-Fickian) diffusion, with a value of *n* as 0.73 for tablets containing MAS-PPN complexes and 0.56 for tablets containing MAS-PPN physical mixture (Table 3) suggesting a shift toward

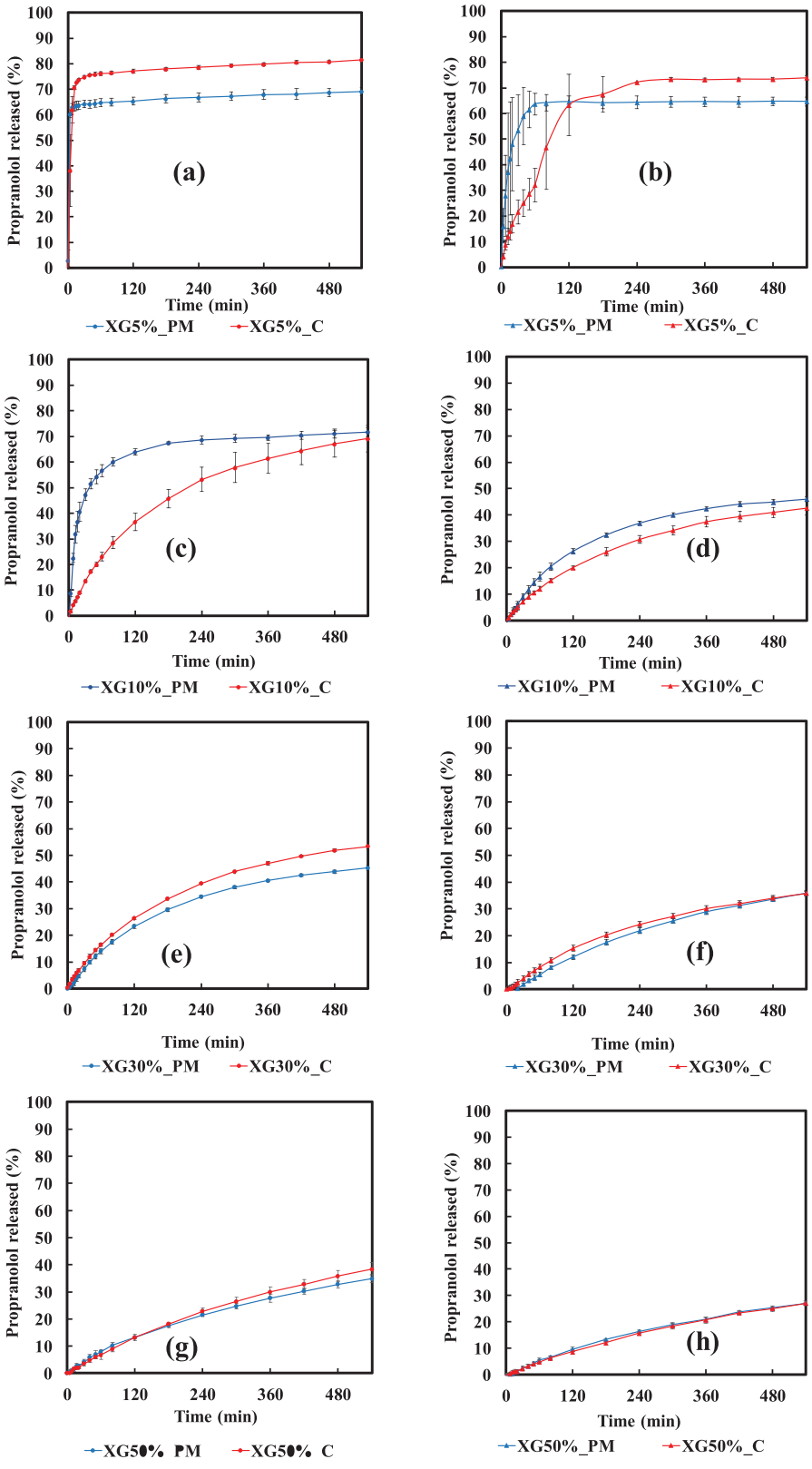

Fig. 4. PPN release profiles from matrices made of MAS-PPN physical mixture and complex particles combined with XG at (a) 5% in pH 1.2, (b) 5% in pH 6.8, (c) 10% in pH 1.2, (d) 10% in pH 6.8, (e) 30% in pH 1.2, (f) 30% in pH 6.8, (g) 50% in pH 1.2, (h) 50% in pH 6.8 over 9 h (n = 3).

swelling kinetics for the complexes. MDT values were similar in acid for tablets containing MAS-PPN complexes (27 min) and those containing MAS-PPN physical mixture (22 min) (Table 3). In buffer, tablets containing MAS-PPN complexes had a considerably higher MDT (76 min), while the tablets containing MAS-PPN physical mixture had a low MDT (19 min). DE values in acid and buffer for tablets containing MAS-PPN physical mixture (67% in acid and 63% in buffer) and for the tablets containing MAS-PPN complexes (78% acid and 67% buffer) suggest the low capability of the tested tablets to modulate PPN release (Table 3). PPN release from tablets containing MAS-PPN complexes was shown to be more controlled in both acid and buffer, compared to PPN release from tablets containing MAS-PPN physical mixture at the 10% w/w XG

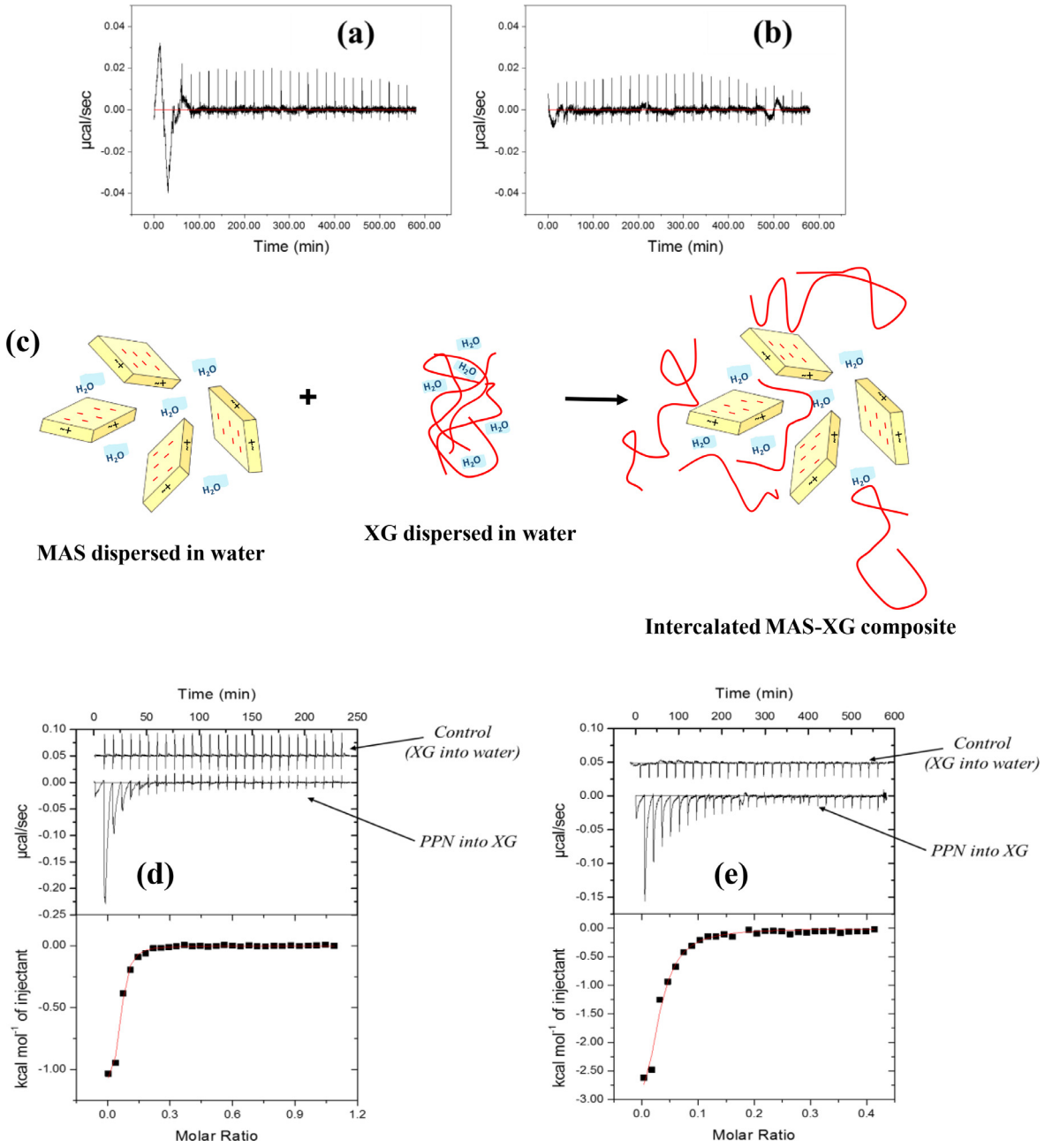

Fig. 5. Raw data for titration of 0.020% w/v XG dispersion (pH 5) into 0.037% w/v MAS dispersion (pH 5) at (a) 25 °C and (b) 37 °C, (c) Scheme of MAS-XG composite formation using MAS dispersed in water and PEO dispersed in water: adapted from (Gao, 2004). Note: Red lines are XG polymer. Calorimetric titration of 0.150% w/v PPN solution (pH 5) into 0.020% w/v XG dispersion (pH 5) at (d) 25 °C and (e) 37 °C. Raw data (top) and integrated heats (bottom) as a function of molar ratio. Control runs suggesting limited interaction between water and XG.

polymer level (Fig. 4c and d). Here again, the *n* value was slightly higher for the tablets containing the MAS-PPN complexes compared to tablets containing MAS-PPN physical mixture in both acidic (0.74 compared to 0.62) and buffer media (0.63 compared to 0.57). This mainly suggests that more PPN was released from the tablets containing MAS-PPN physical mixture which may be due to the compatibility between XG, PPN and MAS. This behavior may be explained in that both XG and MAS may compete for the binding with PPN, possibly leading to a reduction in drug released from the MAS-PPN complexes as it is potentially rebinding with XG. Totea et al. reported using liquid-state analysis of small angle X-ray scattering (SASX), that the generation of a slope of – 2.76 was obtained for just MAS dispersions A considerably different slope of – 3.17 was however obtained for the MAS-PPN complex dispersion. The difference in results was as a result in the difference in structure as a result of the intercalation process. This resulted in the MAS-PPN complex dispersion having a more complex structure (Totea et al., 2020a).

At 30 and 50% w/w XG polymer levels (Fig. 4e-h), there was not much of a difference between the PPN release for MAS-PPN complexes or MAS-PPN physical mixture. In both cases however, there was a considerably higher amount of PPN released in acidic media compared with that of the buffer. This has been explained earlier as the nature of the polymer as well as the effect of ions in the buffer media (Kavanagh & Corrigan, 2004; Mu et al., 2003; Baumgartner, Pavli and Kristl, 2009). Anomalous (non-Fickian) diffusion dominates the kinetics of drug release (Table 3) with the MDT values increasing with an increase in the polymer contents also (Table 3).

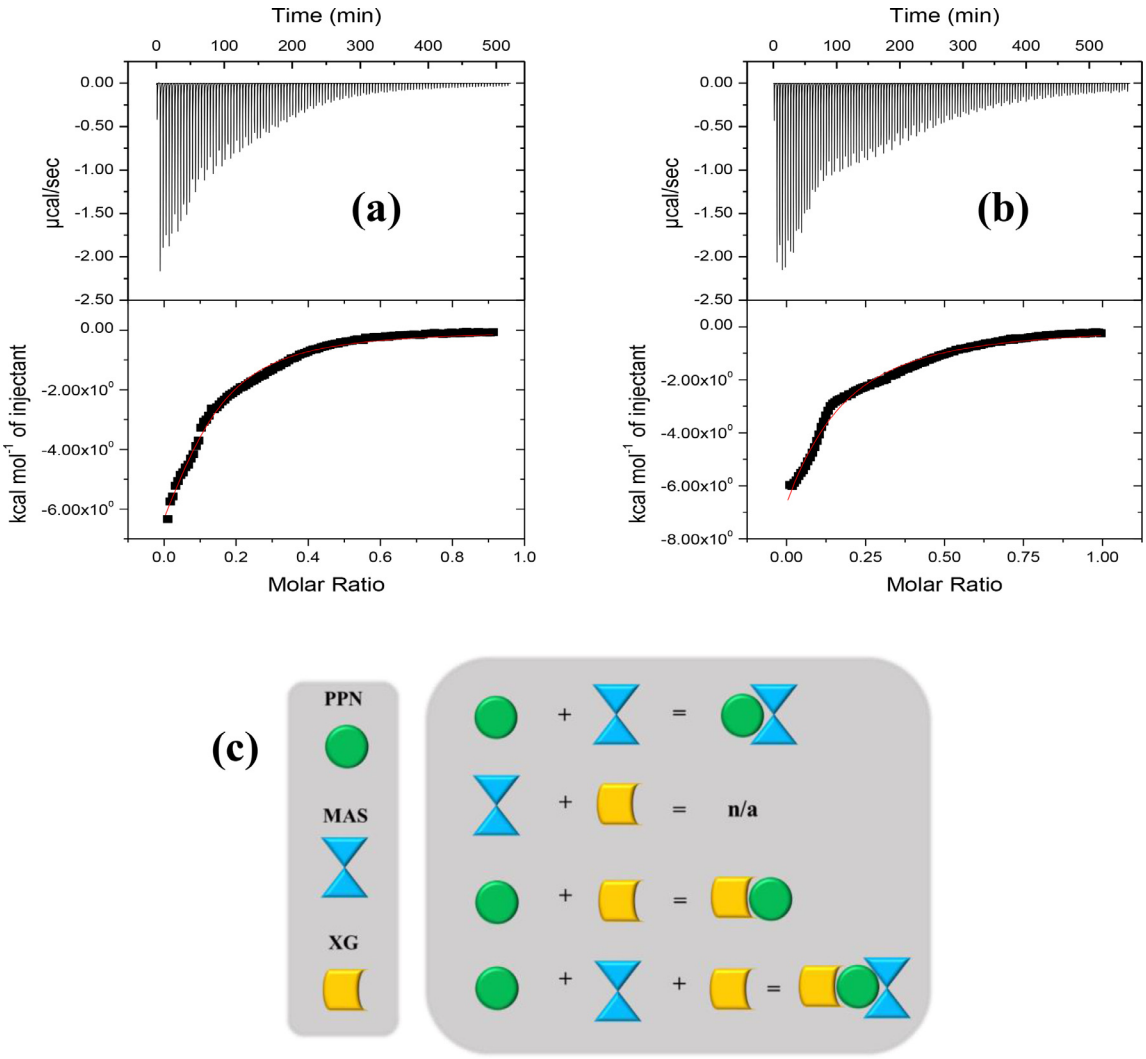

Fig. 6. Titration of 0.150% w/v PPN solution (pH 5) into a mixture of MAS and XG (0.037% w/v MAS; 0.020% w/w XG; pH 5) and thermodynamic profile for adsorption of PPN onto MAS-XG mixture at (a) 25 °C and (b) 37 °C. Raw data (top) and integrated heats (bottom) as a function of molar ratio showing enthalpy (ΔH), entropy(ΔS) or Gibbs free energy (ΔG), (c) schematic representation using shapes of possible chemical interactions between PPN, MAS and XG based on isothermal titration calorimetry results.

3.4. Calorimetric binding studies

SIM and MIM studies for MAS-PPN complexes have been reported by Totea et al., 2019 to be predominantly enthalpically driven from broken and created hydrogen bonds and electrostatic interactions. The focus of this paper is to consider the additional incorporation of XG within the system and report the novel interactions at the molecular level between, MAS and XG, XG and MAS and the adsorption of PPN on MAS-XG complexes.

Following the titration of XG into the MAS dispersion, no interactions were observed between the anionic polysaccharide and the negatively charged MAS. The mixture between MAS and XG was shown to be homogenous with no precipitation being observed in the calorimetric cell at the end of the experiment (Fig. 5a and b) (Vanderbilt Minerals, 2009). The lack of interaction between XG and MAS may lead to very few polymer segments being adsorbed possibly at the platelet edges, with very long polymer tails suspended in solution (Fig. 5c) (Vanderbilt Minerals, 2014).

Binding was observed between PPN (0.150% w/v) and XG (0.020% w/v), which was expected considering the nature of the compounds, i.e. cationic PPN and anionic XG which makes them compatible for intermolecular interactions. Control studies between water at pH 5 and XG dispersion at pH 5 showed very little evidence of binding/self-association through small heats of dilution (Fig. 5d and e). Analysis of the thermodynamic profiles through a 'set of sites' curve fitting revealed that the binding between PPN and XG was enthalpically driven, shown by the negative ΔH and comparatively small -TΔS at both temperatures studied (−5.40 ± 1.90 and −1.52 ± 1.07 kcal/mol at 25 and 37 °C respectively). The increase in experimental temperature from 25 °C to 37 °C led to the binding becoming gradually more enthalpy driven (−1.40 ± 0.26 kcal/mol at 25 °C compared to −6.16 ± 2.11 kcal/mol at 37 °C). The reaction had the same binding energy (ΔG) at both temperatures (−6.80 ± 0.17 kcal/mol at 25 °C and −6.75 ± 0.11 kcal/mol at 37 °C). A slightly higher affinity (K_a) of PPN for XG was observed at 25 °C (97.90 ± 20.4 M), compared to 37 °C (59.10 ± 9.67 M) suggesting more optimal reaction conditions.

Binding between PPN (0.150% w/v (pH 5)) and MAS-XG mixture (0.037% w/v MAS; 0.020% w/w XG; pH 5) led to a different titration profile when compared to the binding between MAS (0.037% w/v) and PPN (0.150% w/v) or the binding between MAS (0.037% w/v) and XG (0.020% w/v) (Fig. 6). This can be related to the competition between MAS and XG for the binding with PPN, as these were both shown to interact with PPN separately. A competitive binding model was fitted to the data using the affinity (K_a) and enthalpy (ΔH) obtained in non-

Table 4
Results showing data analysed through the competitor binding model to calculate affinity (K) and changes in enthalpy (ΔH) and entropy (-TΔS) for the PPN-MAS binding in the presence of XG following multiple injection calorimetric binding studies between PPN (0.150% w/v) and XG-MAS mixture (0.037% w/v MAS; 0.020% w/w XG) at 25 and 37 °C (pH 5). Results are based on three independent repeats.

	25 °C	37 °C
Ka (M)	$3.85 \times 10^6 \pm 6.06 \times 10^5$	$1.37 \times 10^6 \pm 2.19 \times 10^5$
ΔH (kcal/ mol)	-14.50 ± 0.85	-30.30 ± 1.26
-TΔS (kcal/ mol)	-8.84×10^3	-8.55×10^3

competitive binding experiments between PPN and XG at both 25 and 37 °C (Table 4). Results showed that the binding phenomenon between PPN and MAS in the presence of XG was enthalpically driven as shown by the negative enthalpy (ΔH) at both temperatures. The binding affinity (K_a) gradually decreased upon increasing temperature, suggesting that at 25 °C the binding was more energetic ($3.85 \times 10^6 \pm 6.06 \times 10^5$ M at 25 °C and $1.37 \times 10^6 \pm 2.19 \times 10^5$ M at 37 °C). The same behavior was observed between MAS and PPN in a simple MAS-PPN titration experiment as reported by Totea et al., 2019. However it was observed that an increase in affinity between MAS and PPN occurred when XG was added to the reaction ($2.61 \times 10^4 \pm 2.71 \times 10^3$ M 25 °C and $1.48 \times 10^4 \pm 1.48 \times 10^3$ M at 37 °C obtained in the simple MAS-PPN binding studies). Another difference to be noted is that the binding between MAS and PPN is more enthalpically driven in the presence of XG which may be due to the competition for the PPN which affects the binding ((-14.50 ± 0.85 kcal/mol at 25 °C and -30.30 ± 1.26 kcal/mol at 37 °C) obtained in the MAS-PPN binding experiments in the presence of XG, compared to the enthalpy obtained in the simple MAS-PPN binding experiments (-6.03 ± 0.06 kcal/mol at 25 °C and -5.97 ± 1.37 kcal/mol at 37 °C)). Based on the findings concerning the binding reactions taking place between MAS, PPN and XG, a reaction scheme may be proposed (Fig. 6c). This thus explains the dissolution experiments with regards to the PPN release process from the XG matrix tablets containing MAS and PPN physical mix and complex particles.

4. Conclusion

Double loaded MAS-PPN complexes were successfully manufactured and fully characterised using SEM, DSC, XRPD and FTIR. Compacts were prepared using MAS-PPN complexes or physical mixture and dispersed in XG. Bulk compaction behavior was studied for the formulations prepared as plots of relative density vs. upper punch pressure and followed roughly similar trends. The compaction behavior was dominated by plastic recovery during the loading stage following non-reversible deformation, movement and fragmentation of the particles. Dissolution results showed that when using the MAS-PPN complexes, 10% w/w XG polymer level was enough to significantly reduce the burst release experienced by soluble drugs in matrix tablets as well as control the drug release of the model drug propranolol HCl in both acidic and basic media. No binding was observed between XG and MAS at the molecular level using ITC, whereas just as predicted in the hypothesis, PPN was shown to interact with XG. PPN adsorption onto MAS-XG mixture was shown to be influenced by the competition of both MAS and XG for the PPN. This again supports the hypothesis showing the binding phenomenon between PPN and MAS in the presence of XG to be spontaneous and enthalpically driven as shown by the negative enthalpy (ΔH) and comparatively small entropy (-TΔS). This behavior explains the observation from the dissolution testing making the formation of complexes and attractive way of reducing polymer content in matrices.

Declaration of Competing Interest

The authors declare that they have no known competing financial interests or personal relationships that could have appeared to influence the work reported in this paper. This research did not receive any specific grant from funding agencies in the public, commercial, or not-for-profit sectors.

Acknowledgment

Ana-Maria Totea and the authors thank the University of Huddersfield for funding.

Author Contributions

A. M. Totea: Conceptualisation; Data curation; Formal analysis; Methodology; Investigation Writing—Original Draft; Writing—Review & Editing;

I. Dorin; Resources; Software; Validation; Formal analysis; Methodology;

P. R. Laity; Supervision; Validation; Formal analysis; Methodology;

B. R. Conway; Supervision; Methodology;

L. Waters; Supervision; Methodology; Writing—Review & Editing;

K.Asare-Addo; Funding acquisition; Conceptualisation; Formal analysis; Methodology; Writing—Original Draft; Writing—Review & Editing; Supervision;

References

Adebisi, A. O., Conway, B. R., & Asare-Addo, K. (2015). The influence of fillers on theophylline release from clay matrices. *American Journal of Pharmacological Sciences, 3*, 120–125.

Andreopoulos, A. G., & Tarantili, P. A. (2001). Xanthan gum as a carrier for controlled release of drugs. *Journal of Biomaterials Applications, 16*, 34–46.

Asare-Addo, K., Levina, M., Rajabi-Siahboomi, A. R., & Nokhodchi, A. (2011). Effect of ionic strength and pH of dissolution media on theophylline release from hypromellose matrix tablets—Apparatus USP III, simulated fasted and fed conditions. *Carbohydrate Polymers, 86*, 85–93.

Asare-Addo, K., Totea, A. M., & Nokhodchi, A. (2020). Drug release from magnesium aluminium silicate-polyethylene oxide (PEO) nanocomposite matrices: An investigation using the USP III apparatus. *European Journal of Pharmaceutical Sciences, 153*, Article 105474.

Baranauskienė, L., Petrikaitė, V., Matulienė, J., & Matulis, D. (2009). Titration calorimetry standards and the precision of isothermal titration calorimetry data. *International Journal of Molecular Sciences, 10*, 2752–2762.

Baumgartner, S., Pavli, M., & Kristl, J. (2009). Effect of calcium ions on the gelling and drug release characteristics of xanthan matrix tablets. *European Journal of Pharmaceutics and Biopharmaceutics, 69*, 698–707.

Carretero, M. I. (2002). Clay minerals and their beneficial effects upon human health. A review. *Applied Clay Science, 21*, 155–163.

Carretero, M. I., & Pozo, M. (2009). Clay and non-clay minerals in the pharmaceutical industry: Part I. Excipients and medical applications. *Applied Clay Science, 46*, 73–80.

Costa, P., & Lobo, J. M. S. (2001). Modeling and comparison of dissolution profiles. *European Journal of Pharmaceutical Sciences, 13*, 123–133.

CP Kelco KELTROL® / KELZAN® xanthan gum book (pp. 1–28). (2008). CP Kelco. http://www.bisi.cz/cmsres.axd/get/cms$7CVwRhc3USVqgzxkKF96gI$2BChNrXcTq$2BOUdiEtz5TfYA$2B1dJUbBlKfluXdoDfiqojVRVU$2FkQ343xA$3D.

Dash, S., Murthy, P. N., Nath, L., & ChowdhuryKinetic, P. (2010). modeling on drug release from controlled drug delivery systems. *Acta Poloniae Pharmaceutica, 67*, 217–223.

Ferstl, M., Drechsler, M., Rachel, R., Rischer, M., Engel, J., Backofen, M., et al. (2013). The impact of polyelectrolyte structure on the shape of nanoassemblies with cationic peptides. *Journal of Pharmaceutical Sciences, 102*, 2599–2607.

Guan, Y., Zuo, T., Chang, M., Zhang, F., Wei, T., Shao, W., et al. (2015). Propranolol hydrochloride-loaded liposomal gel for transdermal delivery: Characterization and in vivo evaluation. *International Journal of Pharmaceutics, 487*, 135–141.

Han, X., Wang, L., Sun, Y., Liu, X., Liu, W., Du, Y., et al. (2013). Preparation and evaluation of sustained-release diltiazem hydrochloride pellets. *Asian Journal of Pharmaceutical Sciences, 8*, 244–251.

Jian, H., Zhu, L., Zhang, W., Sun, D., & Jiang, J. (2012). Galactomannan (from Gleditsia sinensis Lam.) and xanthan gum matrix tablets for controlled delivery of theophylline: *In vitro* drug release and swelling behavior. *Carbohydrate Polymers, 87*, 2176–2182.

Joshi, G. V., Kevadiya, B. D., Patel, H. A., Bajaj, H. C., & Jasra, R. V. (2009). Montmorillonite as a drug delivery system: Intercalation and *in vitro* release of timolol maleate. *International Journal of Pharmaceutics, 374*, 53–57.

Kanjanakawinkul, W., Rades, T., Puttipipatkhachorn, S., & Pongjanyakul, T. (2013). Nicotine–magnesium aluminum silicate microparticle surface modified with chitosan for mucosal delivery. *Materials Science and Engineering C, 33*, 1727–1736.

Kaur, M., & Datta, M. (2014). Diclofenac sodium adsorption onto montmorillonite: Adsorption equilibrium studies and drug release kinetics. *Adsorption Science & Technology, 32*, 365–387.

Kavanagh, N., & Corrigan, O. I. (2004). Swelling and erosion properties of hydroxypropylmethylcellulose (Hypromellose) matrices—Influence of agitation rate and dissolution medium composition. *International Journal of Pharmaceutics, 279*, 141–152.

Khunawattanakul, W., Puttipipatkhachorn, S., Rades, T., & Pongjanyakul, T. (2010). Chitosan–magnesium aluminum silicate nanocomposite films: Physicochemical characterization and drug permeability. *International Journal of Pharmaceutics, 393*, 220–230.

Laity, P. R., Asare-Addo, K., Sweeney, F., Supuk, E., & Conway, B. R. (2015). Using small-angle X-ray scattering to investigate the compaction behavior of a granulated clay. *Applied Clay Science, 108*, 149–164.

Laity, P. R., & Cameron, R. E. (2008). A small-angle X-ray scattering study of powder compaction. *Powder Technology, 188*, 119–127.

Lazzari, A., Kleinebudde, P., & Knop, K. (2018). Xanthan gum as a rate-controlling polymer for the development of alcohol resistant matrix tablets and mini-tablets. *International Journal of Pharmaceutics, 536*, 440–449.

Meng, N., Zhou, N. L., Zhang, S. Q., & Shen, J. (2009). Synthesis and antimicrobial activities of polymer/montmorillonite–chlorhexidine acetate nanocomposite films. *Applied Clay Science, 42*, 667–670.

Micrometrics Porosity and Its Influence on Pharmaceutical Tablet Dissolution. (1998). *Profiles*. https://www.micromeritics.com/Repository/Files/Porosity-Influence-Pharmaceutical-Tablet-Dissolution-Profiles.pdf.

Mu, X., Tobyn, M. J., & Staniforth, J. N. (2003). Influence of physiological variables on the *in vitro* drug-release behavior of a polysaccharide matrix controlled-release system. *Drug Development and Industrial Pharmacy, 29*, 19–29.

Muśko, M., & Sznitowska, M. (2013). Stability of extemporaneous pediatric oral liquids compounded from tablets and drug substance: Case of propranolol and theophylline. *Acta Poloniae Pharmaceutica, 70*, 137–145.

Nokhodchi, A., Palmer, D., Asare-Addo, K., Levina, M., & Rajabi-Siahboomi, A. (2015). Application of polymer combinations in extended release hydrophilic matrices. *Handbook of Polymers for Pharmaceutical Technologies, 1*, 23–49.

Nunes, C. D., Vaz, P. D., Fernandes, A. C., Ferreira, P., Romao, C. C., & Calhorda, M. J. (2007). Loading and delivery of sertraline using inorganic micro and mesoporous materials. *European Journal of Pharmaceutics and Biopharmaceutics, 66*, 357–365.

Okeke, O. C., & Boateng, J. S. (2016). Composite HPMC and sodium alginate based buccal formulations for nicotine replacement therapy. *International Journal of Biological Macromolecules, 91*, 31–44.

Okeke, O. C., & Boateng, J. S. (2017). Nicotine stabilization in composite sodium alginate based wafers and films for nicotine replacement therapy. *Carbohydrate Polymers, 155*, 78–88.

Park, J. K., Choy, Y. B., Oh, J. M., Kim, J. Y., Hwang, S. J., & Choy, J. H. (2008). Controlled release of donepezil intercalated in smectite clays. *International Journal of Pharmaceutics, 359*, 198–204.

Parolo, M. E., Savini, M. C., Valles, J. M., Baschini, M. T., & Avena, M. J. (2008). Tetracycline adsorption on montmorillonite: PH and ionic strength effects. *Applied Clay Science, 40*, 179–186.

Petri, D. F. (2015). Xanthan gum: A versatile biopolymer for biomedical and technological applications. *Journal of Applied Polymer Science, 23*, 132. doi: 10.1002/app.42035.

Pongjanyakul, T., Khunawattanakul, W., & Puttipipatkhachorn, S. (2009). Physicochemical characterizations and release studies of nicotine–magnesium aluminum silicate complexes. *Applied Clay Science, 44*, 242–250.

Pongjanyakul, T., & Rojtanatanya, S. (2012). Use of propranolol-magnesium aluminium silicate intercalated complexes as drug reservoirs in polymeric matrix tablets. *Indian Journal of Pharmaceutical Sciences, 74*, 292.

Rapacz-Kmita, A., Krupa, A., & Jachowicz, R. (2010). Preliminary approach to application of modified smectite clay to form tablets in direct compression process. *Materiały Ceramiczne, 62*, 366–368.

Riippi, M. (2018). Dependence between dissolution rate and porosity of compressed erythromycin acistrate tablets. *European Journal of Pharmaceutics and Biopharmaceutics, 46*, 169–175.

Ritger, P. L., & Peppas, N. A. (1987). A simple equation for description of solute release I. Fickian and non-Fickian release from non-swellable devices in the form of slabs, spheres, cylinders or discs. *Journal of Controlled Release, 5*, 23–36.

Rojtanatanya, S., & Pongjanyakul, T. (2010). Propranolol–magnesium aluminum silicate complex dispersions and particles: Characterization and factors influencing drug release. *International Journal of Pharmaceutics, 383*, 106–115.

Romero, A. I., Villegas, M., Cid, A. G., Parentis, M. L., Gonzo, E. E., & Bermúdez, J. M. (2018). Validation of kinetic modeling of progesterone release from polymeric membranes. *Asian Journal of Pharmaceutical Sciences, 13*, 54–62.

Rongthong, T., Sungthongjeen, S., Siepmann, J., & Pongjanyakul Quaternary, T. (2013). polymethacrylate–magnesium aluminum silicate films: Molecular interactions, mechanical properties and tackiness. *International Journal of Pharmaceutics, 458*, 57–64.

Siahi-Shadbad, M. R., Asare-Addo, K., Azizian, K., Hassanzadeh, D., & Nokhodchi, A. (2011). Release behavior of propranolol HCl from hydrophilic matrix tablets containing psyllium powder in combination with hydrophilic polymers. *AAPS PharmSciTech, 12*, 1176–1182.

Sinha Ray, S., Maiti, M., Okamoto, K., & Yamada, K. (2002). Ueda New polylactide/layered silicate nanocomposites. 1. Preparation, characterization, and properties. *Macromolecules, 35*, 3104–3110.

Talukdar, M. M., & Kinget, R. (1995). Swelling and drug release behavior of xanthan gum matrix tablets. *International Journal of Pharmaceutics, 120*, 63–72.

Talukdar, M. M., Michoel, A., Rombaut, P., & Kinget, R. (1996). Comparative study on xanthan gum and hydroxypropylmethyl cellulose as matrices for controlled-release drug delivery I. Compaction and in vitro drug release behavior. *International Journal of Pharmaceutics, 129*, 233–241.

Totea, A. M., Dorin, I., Gavrilov, G., Laity, P. R., Conway, B. R., Waters, L., et al. (2019). Real time calorimetric characterisation of clay–drug complex dispersions and particles. *International Journal of Pharmaceutics: X, 1* Article: 100003.

Totea, A. M., Dorin, I., Laity, P. R., Sabin, J., Conway, B. R., Waters, L., et al. (2020a). A molecular understanding of magnesium aluminium silicate–drug, drug-polymer, magnesium aluminium silicate-polymer nanocomposite complex interactions in modulating drug release: Towards zero order release. *European Journal of Pharmaceutics and Biopharmaceutics, 154*, 270–282.

Totea, A. M., Sabin, J., Dorin, I., Hemming, K., Laity, P. R., Conway, B. R., et al. (2020b). Thermodynamics of clay–drug complex dispersions: Isothermal titration calorimetry and high-performance liquid chromatography. *Journal of Pharmaceutical Analysis, 10*, 78–85.

Trivedi, V., U, Nandi, Maniruzzaman, M., & Coleman, N. J. (2018). Intercalated theophylline-smectite hybrid for pH-mediated delivery. *Drug Delivery and Translational Research, 8*, 1781–1789.

Vanderbilt Minerals VANZAN Xanthan Gum (2009), pp. 1–12. (Vanderbilt Minerals). https://www.vanderbiltminerals.com/resources/VANZAN_Brochure_English_Web.pdf

Vanderbilt Minerals, VEEGUM (2014). *Magnesium Aluminum Silicate VANATURAL Bentonite Clay For Personal Care and Pharmaceuticals What They Are* (pp. 1–27). Vanderbilt Minerals. https://www.vanderbiltminerals.com/resources/VEEGUM_VANATURAL_P_C_Pharma_Web.pdf.

Wang, Z., Wu, J., Zhu, L., & Zhan, X. (2016). Activation of glycerol metabolism in Xanthomonas campestris by adaptive evolution to produce a high-transparency and low-viscosity xanthan gum from glycerol. *Bioresource Technology, 211*, 390–397.

Wang, Z., Wu, J., Zhu, L., & Zhan, X. (2017). Characterization of xanthan gum produced from glycerol by a mutant strain Xanthomonas campestris CCTCC M2015714. *Carbohydrate Polymers, 157*, 521–526.